Lasers in Manufacturing Conference 2019

The use of a ns-pulsed, high repetition rate green laser for SLM of 99.9% pure Cu

Ali Gökhan Demir[a*], Metto Colopi[a], Barbara Previtali[a]

[a]*Department of Mechanical Engineering, Politecnico di Milano, Via La Masa 1, 20158 Milan, Italy*

Abstract

The most common laser type used in selective laser melting (SLM) machines is continuous fiber laser emitting at 1 μm. The low optical absorptivity of Cu to ~1 μm wavelength renders pure Cu a highly demanding material for SLM. The low optical absorptivity along with high thermal conductivity causes unstable processing conditions when standard SLM machine are used with pure Cu. Conversely, Cu has a much higher optical absorptivity at the green wavelength. Until recently, high power green lasers have not been available for material processing. This work investigates the use of a novel ns-pulsed fiber laser operating at the second harmonic (532 nm) for SLM of 99.9% pure Cu powder. In particular, the laser source operates at 30 MHz repetition rate providing ns regime and up to 110 W average power. The green laser is implemented to a bespoke open SLM platform. Results show that cubic specimens with densities >99.5% could be achieved.

Keywords: Selective laser melting; pure Cu; green laser; porosity

1. Introduction

Copper and its alloys are highly appealing for their electrical and thermal conductivity for various applications ranging from high power electronics, energy, aerospace, and automotive. Combined with the geometrical flexibility of additive manufacturing processes, novel products, with enhanced thermal and electrical performance, can be potentially produced employing Cu and its alloys. Copper is highly reflective to wavelengths in infrared and near infrared regions (see Fig.1), while the absorptivity becomes 30-35% and 45-50 % at green (532nm) and blue wavelengths respectively (Steen and J., 2010). Resultantly, the laser

* Corresponding author. Tel.: +39-022-399-8590; fax: +39-022-399-8585.
E-mail address: aligokhan.demir@polimi.it.

processing of Cu alloys has been problematic. The relatively recent introduction of high power and high brilliance fiber and disc lasers, and diode lasers with shorter wavelengths has extended the processability of Cu alloys laser cutting and welding operations. This opened up the possibility of using these sources also for processing Cu and its alloys via selective laser melting (SLM). Given the SLM requirements of a small beam spot for high precision, near infrared lasers have remained limited to the use of the single mode fiber lasers with moderate power outputs. However, SLM differs greatly in terms of prolonged process duration, hence being prone to defect formation. Today, the processing of Cu alloys remains limited due to the high reflectivity at the standard wavelength of the fiber lasers employed in the SLM machines and its high thermal conductivity.

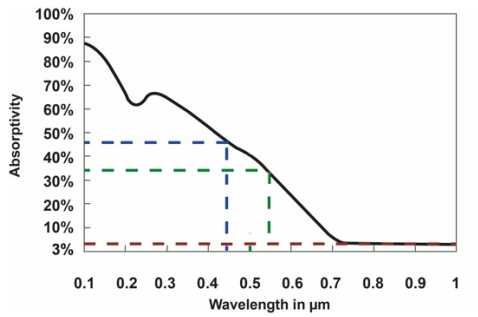

Fig.1. Optical absorptivity of pure Cu at different wavelengths. Adapted from (Steen and Mazumder, 2010).

Table 1. The state of the art in SLM of pure Cu along with principal characteristics of used laser and properties of the consolidated part.

Reference	Cu purity	Laser source	Wavelength (nm)	Emission mode	Max laser power	Max apparent density	Indicative build rate (cm^3/h)
Pogson et al., 2003	N/A	Nd:YAG	1064	PW (80-160 ns)	90 W Average	N/A	0.5
Lykov et al., 2016	N/A	Fiber	1070	PW (100-400 µs)	200 W	>99%	3.15
Kaden et al., 2017	99%	Fiber	1030	PW (500 fs)	20 W Average	N/A	1.1
Trevisan et al., 2017	99.96%	Fiber	1070	CW	200 W	83%	3.5
Masuno et al., 2017	N/A	Blue diode	450	CW	100 W	N/A	N/A
Ikeshoji et al., 2018	99.90%	Fiber	1070	CW	1000 W	96.6%	5.4
Colopi et al., 2018	99.90%	Fiber	1070	CW	1000 W	97.8%	12.6
Jadhav et al., 2019	99.95%	Fiber	1080	CW	1000 W	>98%	3.9
Tiberto et al., 2019	N/A	Nd:YAG	1070	CW	100 W	74%	3

The processability of pure Cu via SLM has received an increasing attention over the last few years. Table 1 summarizes the state of the art in SLM of pure Cu. To overcome mainly the optical absorption limits of the material, several options have been employed, that combine wavelength, emission mode (continuous wave/CW, pulsed wave/PW), and different power levels. It can be seen that the first attempts date back to 2003 where the employed solution was a ns-pulsed Nd:YAG source (Pogson et al., 2003). In the more recent years the use of the common single mode fiber laser source with low power levels has been demonstrated to be insufficient for high density components (Trevisan et al., 2017). The research later on followed onto

different solutions over the SLM system. Lykov et al. (2016) suggested the use of preheating to improve densification behaviour. A group of researchers investigated a high power fiber laser with power levels reaching 1 kW (Colopi et al., 2018; Ikeshoji et al., 2018; Jadhav et al., 2019). The results showed that the high CW power activates the non-linear optical absorption behaviour of Cu by generating molten phase, which in return has a higher absorption compared to the solid. All authors, however, observed instabilities due to high thermal conductivity. Kaden et al., (2017) showed the feasibility of producing highly detailed structures by using a fs-pulsed laser.

A less explored pathway concerns the use of shorter laser wavelengths. Masuno et al. (2017) showed the use of a blue diode laser operating at 450 nm wavelength for SLM of pure Cu. Due to the low brilliance of the diode, the blue laser after being launched into a transmissive fiber, was focused at a 200 spot size μm, which is larger than common spot sizes in SLM (range of 30-100 μm). Moreover, blue wavelength lasers are not widely available in the market. There is also a scarcity of optical elements with coating resistant to this short wavelengths.

To authors' knowledge no previous scientific work to date has explored the use of green laser configuration in SLM. On the other hand, it is known that Fraunhofer Institute for Laser Technology ILT has announced in the "SLM in Green" national project the development of a 400 W CW green laser intentionally for SLM of Cu (Fraunhofer ILT, 2017). Moreover, Trumpf has showcased a new green disk laser with pulse function connected to the TruPrint 1000 SLM machine (Trumpf, 2018).

Therefore, this work aims to investigate the use of a novel high average power, ns-pulsed green laser with MHz pulse repetition rate for SLM of pure Cu powder. The work shows system components and integration as well as experimental work confirming the suitability of this laser type for producing pure Cu components with high density. The results show that even at moderate average power levels apparent density levels higher than 99.5% could be achieved.

2. Experimental setup

2.1. Material

Gas atomized pure copper powder (Cu 99.9%wt, O 0.08%wt, P <0.15%wt) was used throughout the work (LPW Technology Ltd, Runcorn, UK). The powder particle size was +15 μm/-45 μm. Base plate materials was AISI 316L stainless steel (Cr 16-18 wt%, Ni 10-14 wt%, Mo 2-3 wt%, Mn 2 wt%; C <0.03 wt%, Fe bal).

2.2. Laser source

The laser source employed in this study was a pulsed active fiber laser with second harmonic generation (GLPN-100-M, IPG Photonics, Cambridge, USA). The laser was configured with a remote amplifier, which also encased a second harmonic generator, providing an output wavelength of 532 nm. The laser emitted at a fixed repetition rate (PRR) of 30 MHz with a pulse duration (τ) of 1.4 ns. The average output power was regulated in automatic power control mode by varying the input power level (P%). The output power was measured by means of a calorimetric power meter (W-3000-D55-HPB-RS, Laserpoint, Vimodrone, Italy). The resultant power curve is almost constant as a function of the commanded power level as reported in Fig.2a. The pulse energy (E_p) was calculated following the simple relationship:

$$E_p = P_{avg}/PRR \qquad (1)$$

On the other hand pulse peak power (P_{peak}) was estimated using the following relationship:

$$P_{peak} = E_p/\tau \quad (2)$$

The handling of the high power laser beam was a special concern, where an optical chain able to withstand the high brilliance of the green laser was configured. The laser provided a divergent beam at the output, which was collimated by a 255 mm lens to a beam size of approximately 6 mm. The beam was launched to a scanner head (Superscan II, Raylase, Wessling, Germany) with focus shifting optics (Focusshifter, Raylase, Wessling, Germany). The laser beam was focused with an f-theta lens with 260 mm focal length (SL-532-165-260, Wavelength Technologies). The laser beam size was measured with a beam profiler (Beamage USB 3.0, Gentec, Quebec, Canada) with 5.5 μm pixel size (Fig.2b). The minimum spot diameter ($1/e^2$) at the nominal focal point of the focusing lens was as 38 μm. The beam quality factor was also determined for this configuration as M^2=1.25.

Table 2. The main characteristics of the employed laser source.

Parameter	Value
Wavelength, λ	532 nm
Maximum average power, $P_{avg,max}$	110 W
Maximum pulse energy, $E_{p,max}$	3.6 μJ
Maximum pulse peak power, $P_{peak,max}$	2.6 kW
Pulse repetition rate, PRR	30 MHz
Beam quality factor, M^2	1.25
Pulse duration, τ	1.4 ns
Minimum spot diameter, d_0	38 μm

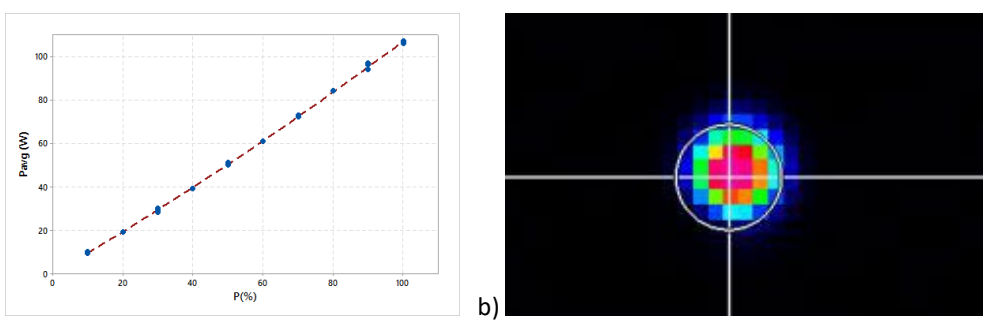

Fig.2. (a) Measured average power output of the laser as a function of power control level. (b) Measured beam profile (d_0=38 μm).

2.3. Open SLM platform

Selective laser melting process was performed employing an open SLM system developed in-house namely Powderful (Fig.3). The mechanical system consisted of a custom-made powder bed able to process a small quantity of powder (<500 g), which was placed in a sealed chamber. The build plate size was 60x60x20 allowing to build simple sample geometries suited especially for new material development. Prior to processing an inertization procedure was carried out, where a cycle of vacuum down to -950 mbar and Ar

purging up to 10 mbar was applied twice (Caprio et al., 2017; Demir et al., 2017). The system automation was carried out in Labview environment (National Instruments, Austin, TX, USA).

Fig.3. The integrated SLM system. (a) Remote amplifier of the laser source, (b) collimating unit, (c) scanner head, (d) f-theta lens, (e) protective window, (f) powder-bed.

2.4. Experimental plan

After initial tests, not reported here for the sake of brevity, an experimental plan with three main process parameters, namely average laser power (P_{avg}), scan speed (v) and hatch distance (h), was carried out. Average laser power was varied at moderate levels of 40 and 50 W, which provided peak power levels of approximately 200 and 250 W respectively. Scan speeds were chosen at 400, 500, and 600 mm/s. Hatch distance was varied at values comparable to the beam size between 0.03, 0.05, and 0.07 mm. The focal position was kept on the powder bed surface and the z-axis of the scanner was kept at its neutral position. Thus, the minimum spot diameter at the focal plane of the f-theta lens could be employed. Layer thickness was fixed at 50 μm. The base plate was AISI 316L in order to reduce the heat losses due to conduction with the base plate (Colopi et al., 2018). Cubic samples with 5x5x5 mm^3 dimensions were produced. Hatch pattern was rotated at 45° at each layer. Three replications were produced for all conditions and the runs were executed in a random order. The details of the experimental plan are reported in Table 3.

Specimens were separated from the base plate, cut, mounted in resin and polished. Optical microscope images were taken of the entire specimens. Apparent density was measured over the obtained photographs by means of image processing software, defined as:

$$\rho_A = \frac{A_{tot} - A_{pore}}{A_{tot}} \qquad (3)$$

where A_{tot} and A_{pore} are the total area and the total pore area measured over the cross section images. Border porosity was not considered at this stage, since the border parameters were not studied within this work. The results were analysed as a function of energy density defined as:

$$E = \frac{P_{avg}}{v \cdot h \cdot z} \quad (4)$$

Table 3. The details of the employed experimental plan.

Fixed parameters	
Hatch rotation angle, α (°)	45
Layer thickness, z (μm)	50
Process gas	Ar
Base plate	AISI316L
Varied parameters	
Average laser power, P_{avg} (W)	40; 50
Scan speed, v (mm/s)	400; 500; 600
Hatch distance, h (mm)	0.03; 0.05;0.07

3. Results

3.1. Feasibility window

Fig.4 reports the samples built on the base plate. In an initial stage, the results were evaluated as a function of process feasibility. Two different types of defects were observed: i) no proper adhesion to the base plate; ii) delamination between built layers. It was noticed that the reduction of average power results in a less stable process window overall. It should be noted that the peak power of the pulses decay from approximately 1.2 kW to 0.95 kW, when the average power is reduced from 50 W to 40 W. It can be inferred that pure Cu is sensitive to peak power variations. Due to the enhanced absorption at the green wavelength, it can be expected that this sensitivity remains due to the high thermal conductivity of the material.

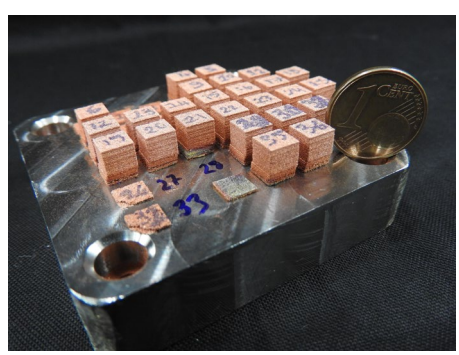

Fig. 4. The built specimens.

3.2. Apparent density

Fig.5a shows the apparent density measurements as a function of energy density divided into the average power classes. The graph also compares the results of the present work with the data available in literature.

The apparent density follows a variable trend over the employed energy density range. The distinction between 40 W and 50 W in terms of densification behaviour is evident. The process stability is higher with the 50 W average power condition. Fig 5b compares the results at the high density range between 95 and 100%. It can be seen that the highest densities achieved in literature. Concerning the samples produced at 50 W, the density levels exceed what has been observed with high power single mode fiber lasers (Colopi et al., 2018; Ikeshoji et al., 2018; Jadhav et al., 2019). It can also be noted that the energy density levels required in this work are only a fraction of those employed in literature underlying the improved process efficiency and hence productivity.

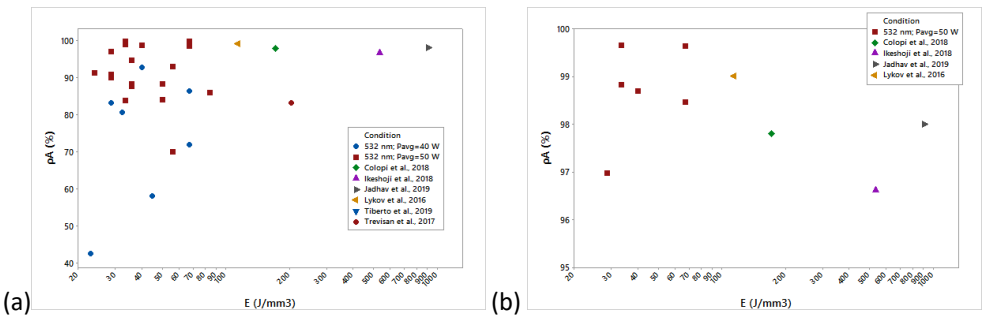

Fig. 5. Comparison of apparent density obtained with the data available in literature (a) the complete density ranges observed; (b) the density range between 95-100%..

Fig.6 shows example of cross-section section images obtained with 50 W average power. It can be seen that the pores at low energy densities are large in size and propagate between layers. Such conditions are related to lack of fusion defects. Increased energy density shows significant improvement of the density as the pore quantity and size decrease drastically. At 66 J/mm^3 samples with apparent density of 99.6% were achieved in a stable manner. At this configuration the theoretical build rate was calculated as 2.7 cm^3/h. Concerning the power availability of the employed laser source a more extended work is expected to produce sufficient density at higher build rates.

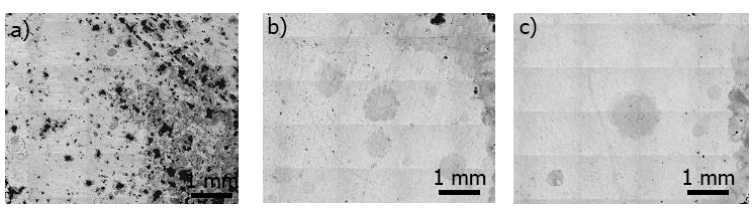

Fig. 6. Cross-section images of samples produced with (a); P_{avg}= 50 W, v=600 mm/s, h=0.07 mm, E=24 J/mm^3, ρ_A=91.1% (b) P_{avg}= 50 W, v=600 mm/s, h=0.05 mm, E=33 J/mm^3, ρ_A=99.6%; (c) P_{avg}= 50 W, v=500 mm/s, h=0.03 mm, E=66 J/mm^3, ρ_A=99.6%.

4. Conclusions

The present work reported the SLM of 99.9% pure Cu with a novel ns-pulsed high average power green fiber laser. The paper focused on the system development as well as process feasibility. The initial results showed the feasibility of processing pure Cu powders with density levels exceeding 99.5%. The instable densification behaviour over the explored energy density regime required further attention concerning the laser emission behaviour. Future works will address an extended study of process parameters as well as the

optical absorption behaviour during the process.

Acknowledgements

The authors acknowledge Mr. Ashutosh Singh and Mr. Kenan Kaan Yetil for their support during the experimental activity. The authors gratefully acknowledge IPG Italy for the longstanding collaboration. The authors wish to express their gratitude to Raylase for employed scanner head. Optoprim Srl is thanked for the technical support. This work was supported by European Union, Repubblica Italiana, Regione Lombardia and FESR for the project MADE4LO under the call "POR FESR 2014-2020 ASSE I - AZIONE I.1.B.1.3".

References

Caprio, L., Demir, A.G., Previtali, B., 2017. Comparative study between CW and PW emissions in selective laser melting, in: 36th International Congress on Applications of Lasers & Electro-Optics ICALEO. p. 1304.

Colopi, M., Caprio, L., Demir, A.G., Previtali, B., 2018. Selective laser melting of pure Cu with a 1 kW single mode fiber laser. Procedia CIRP 74, 59–63. doi:10.1016/j.procir.2018.08.030

Demir, A.G., Monguzzi, L., Previtali, B., 2017. Selective laser melting of pure Zn with high density for biodegradable implant manufacturing. Addit. Manuf. 15, 20–28. doi:10.1016/j.addma.2017.03.004

Fraunhofer ILT, 2017. Green Light for New 3D Printing Process [WWW Document]. URL https://www.ilt.fraunhofer.de/en/press/press-releases/press-release-2017/press-release-2017-08-30.html

Ikeshoji, T.T., Nakamura, K., Yonehara, M., Imai, K., Kyogoku, H., 2018. Selective Laser Melting of Pure Copper. Jom 70, 396–400. doi:10.1007/s11837-017-2695-x

Jadhav, S.D., Dadbakhsh, S., Goossens, L., Kruth, J.-P., Van Humbeeck, J., Vanmeensel, K., 2019. Influence of selective laser melting process parameters on texture evolution in pure copper - Manuscript submitted for publication. J. Mater. Process. Technol. 270, 47–58. doi:10.1016/j.jmatprotec.2019.02.022

Kaden, L., Matthäus, G., Ullsperger, T., Engelhardt, H., Rettenmayr, M., Tünnermann, A., Nolte, S., 2017. Selective laser melting of copper using ultrashort laser pulses. Appl. Phys. A Mater. Sci. Process. 123, 1–6. doi:10.1007/s00339-017-1189-6

Lykov, P., Baytimerov, R., Vaulin, S., Safonov, E., Zherebtsov, D., 2016. Selective Laser Melting of Copper by 200 W CO2 Laser. SAE Tech. Pap. Ser. 1, 2–5. doi:10.4271/2016-01-0333

Masuno, S., Tsukamoto, M., Tojo, K., Keita;, A., Funada, Y., Yu, S., 2017. Metal powder bed fusion additive manufacturing with 100 W blue diode laser. 36th Int. Congr. Appl. Lasers Electro-Optics ICALEO 4–5.

Pogson, S.R., Fox, P., Sutcliffe, C.J., O'Neill, W., 2003. The production of copper parts using DMLR. Rapid Prototyp. J. 9, 334–343. doi:10.1108/13552540310502239

Steen, W.M., J., M., 2010. Laser Material Processing, Springer-Verlag London Limited. doi:10.1007/978-1-84996-062-5

Steen, W.M., Mazumder, J., 2010. Laser Material Processing, Media. Springer London, London. doi:10.1007/978-1-84996-062-5

Tiberto, D., Klotz, U.E., Held, F., Wolf, G., 2019. Additive manufacturing of copper alloys: influence of process parameters and alloying elements. Mater. Sci. Technol. 35, 969–977. doi:10.1080/02670836.2019.1600840

Trevisan, F., Calignano, F., Lorusso, M., Manfredi, D., Fino, P., 2017. Selective laser melting of chemical pure copper powders, in: Euro PM 2017. Milan.

Trumpf, 2018. World premiere at Formnext: green laser from TRUMPF prints copper and gold [WWW Document]. URL https://www.trumpf.com/it_IT/impresa/stampa/comunicatistampa/comunicato-stampa-pagina-con-i-dettagli/release/world-premiere-at-formnext-green-laser-from-trumpf-prints-copper-and-gold/